Proceedings of the 17th World Congress
The International Federation of Automatic Control
Seoul, Korea, July 6-11, 2008

Robust Consistency-Based Diagnosis of Nonlinear Systems by Set Observation

F. Wolff, P. Krutina and V. Krebs

Institut für Regelungs- und Steuerungssysteme
Universität Karlsruhe (TH), Germany
phone: +49 (721) 608-2467, fax: +49(721) 608-2707
e-mail: {wolff,krebs}@irs.uni-karlsruhe.de

Abstract: Achieving robustness and a high fault sensitivity simultaneously is one of the most important goals of diagnosis system design. The idea of the so-called passive approach, which has been given relatively little attention in literature so far, is to include the effects of measurement and model uncertainties in the residual. In the subsequent residual evaluation, these uncertainties can then be accounted for such that false alarms can be precluded.
Following this passive approach, we present a new model-based diagnosis algorithm based on state-set observation of nonlinear continuous-time systems. A set-valued observer following the well-known predictor-corrector scheme is used to calculate a set of system states. These sets are consistent with the underlying system model as well as with the discrete measurements including both model and measurement uncertainties. In the prediction step, a validated ODE solving method is applied for calculation of the consistent state set. To the authors knowledge, such a nonlinear continuous-time set-valued observer has not yet been used for diagnosis tasks. The performance of the method is demonstrated using measured data of fault-free and faulty operation of an inverted pendulum as a benchmark system.

Keywords: Fault detection and diagnosis; Continuous-time system estimation; Nonlinear systems; Nonlinear observer and filter design; Robust estimation; Uncertainty descriptions.

1. INTRODUCTION

The growing complexity of technical systems results in an increasing demand for efficient fault diagnosis methods that allow safe and reliable operation of the system. Therefore, the aim of a diagnosis system is to detect faults as early as possible while, at the same time, false alarms, e.g. due to measurement noise, must be avoided to minimize unnecessary system shutdowns. Hence, achieving robustness and a high fault sensitivity simultaneously is one of the most important goals of diagnosis system design.

Model-based diagnosis methods often perform better than signal-based approaches. Therefore, they are the subject of intensive research activities (see e.g. Chen and Patton (1999); Patton et al. (2000); Planchon (2007)). In model-based diagnosis, mathematical system models can be used to produce analytical redundancy. With help of this redundancy, residuals are created that show a characteristic response to certain system faults. Thus, they allow not only *fault detection*, but also separation of different faults, commonly known as *fault isolation*. The diagnosis system should perform this fault detection and isolation (FDI) task despite measurement uncertainties or incomplete system knowledge resulting in an imprecise system model.

Towards this goal, two different approaches can be distinguished. The *active approach* aims at generating residuals which are sensitive to faults, while effects of disturbances not representing faulty system behavior are suppressed as far as possible. *Unknown input oberservers* or *parity equations* are well-known and extensively studied methods following the active approach. An excellent survey of such active methods can be found in Patton et al. (2000). However, the desired decoupling of the residuals from the disturbances can usually be achieved only approximately due to inevitable modeling errors.

The *passive approach*, on the other hand, aims at generating residuals such that the effects of measurement and model uncertainties can be accounted for in the subsequent residual evaluation stage of the diagnosis algorithm. Using appropriate system models, e.g. interval models, and state-set observation techniques, uncertainties in both measurements and system models can be considered. A good overview of robustness issues in active and passive approaches can be found in Puig et al. (2000).

Instead of checking whether the generated residual exceeds a given threshold, the real system behavior given by measurements and the modeled system behavior are checked for consistency. This approach is therefore called *consistency-based diagnosis* and is particularly well suited to work with set-valued observers.

A number of publications deal with the design of set-valued observers for both, linear and nonlinear dynamic systems, using a variety of different set descriptions such as polytopes, intervals or ellipsoids (see e.g. Jaulin et al. (2001); Shamma and Tu (1997); Puig et al. (2002); Hanebeck (2001); Planchon (2007)). However, in most cases discrete-time dynamic systems are considered while continuous-

time systems are rarely used. Since an exact discrete-time model cannot be calculated for most nonlinear continuous-time systems, such approaches can only lead to approximate state sets. The continuous-time approach allows the calculation of state sets that are guaranteed to enclose the true state sets. Furthermore, to the authors knowledge, nonlinear continuous-time set-valued observers have not yet been used for a consistency-based diagnosis algorithm although the guaranteed inclusion property can be used beneficially to obtain robust diagnosis results.

In this contribution, we describe a new diagnosis algorithm for continuous-time nonlinear systems using state-set observers. By using system models whose parameters are allowed to vary within a given interval as well as measurements including unknown-but-bounded measurement uncertainty, we yield a *robust consistency-based diagnosis algorithm* for faults whose effects can be described by changes in the system parameters.

The paper is organized as follows: After introducing some notation in Section 2, we describe the nonlinear state-set observer in Section 3. The diagnosis algorithm comprising the state-set observer and the subsequent evaluation of the calculated state sets is described in Section 4. In Section 5, the performance of the method is demonstrated using real measurement data from an inverted pendulum. The contribution is completed with the conclusions in Section 6.

2. NOTATION

In this section, we give a short overview of interval arithmetic notation and the type of system models considered in this contribution.

2.1 Interval Arithmetic

A real interval is defined as the set of real numbers

$$[a] = \left[a^-, a^+\right] = \left\{x \,|\, a^- \leq x \leq a^+;\, a^-, x, a^+ \in \mathbb{R}\right\}. \quad (1)$$

The set of all real intervals is denoted by $\mathbb{IR}$. The basic interval arithmetic operations are defined by

$$[a] \circ [b] = \{x \circ y \,|\, x \in [a]\,,\, y \in [b]\} \quad (2)$$

with $\circ \in \{+, -, *, /\}$ and $0 \notin [b]$ if $\circ = /$. Functions of intervals are defined as

$$[f([a])] = \{y \,|\, \min f(x) \leq y \leq \max f(x),\, x \in [a]\}. \quad (3)$$

The midpoint and the width of $[a]$ are denoted by $\hat{a}$ and $w\{[a]\}$, respectively. The intersection of two intervals is the usual set intersection

$$[a] \cap [b] = \{x \,|\, x \in [a] \wedge x \in [b]\}. \quad (4)$$

Vectors and matrices are written in bold face, the n-dimensional identity matrix is denoted by $\boldsymbol{I}_n$. Interval vectors $[\boldsymbol{a}]$ or matrices $[\boldsymbol{A}]$ are vectors or matrices built of interval components. Operations like width, midpoint and intersection of interval vectors or matrices are defined componentwise.

Note that interval arithmetic operations can be implemented such that roundoff errors are included in the result interval. The exact result is then guaranteed to be contained in the calculated intervals. Further information about interval arithmetic, its properties and implementation issues can e.g. be found in Jaulin et al. (2001).

2.2 System Models

We consider uncertain, continuous-time nonlinear systems of order n in state space

$$\mathcal{M} = \begin{cases} [\dot{\boldsymbol{x}}] & = [\boldsymbol{f}([\boldsymbol{x}]\,,[\boldsymbol{u}])] \\ [\boldsymbol{y}] & = ([x_1]\,,[x_2]\,,\ldots,[x_q])^{\mathrm{T}} \end{cases} \quad (5)$$

with the interval state vector $[\boldsymbol{x}] \in \mathbb{IR}^n$, the interval input vector $[\boldsymbol{u}] \in \mathbb{IR}^p$ and the interval output vector $[\boldsymbol{y}] \in \mathbb{IR}^q$. For simplicity of the subsequent arguments, we assume $q \leq n$. The system function $[\boldsymbol{f}(\cdot)]$ is required to be a sufficiently smooth nonlinear function. Furthermore, we restrict our considerations to the case of systems with linear output equations, a requirement which is fulfilled by a wide class of technical systems. By using a regular linear transformation, any system model with a linear output equation can be converted into the form given by (5).

Since $[\boldsymbol{u}]$ and $[\boldsymbol{y}]$ are vectors of intervals rather than real numbers, we can take unknown-but-bounded measurement uncertainties $\Delta\boldsymbol{u}$ and $\Delta\boldsymbol{y}$ into account:

$$[\boldsymbol{u}] = [\boldsymbol{u}_{\mathrm{meas}} - \Delta\boldsymbol{u}, \boldsymbol{u}_{\mathrm{meas}} + \Delta\boldsymbol{u}] \quad (6)$$

$$[\boldsymbol{y}] = [\boldsymbol{y}_{\mathrm{meas}} - \Delta\boldsymbol{y}, \boldsymbol{y}_{\mathrm{meas}} + \Delta\boldsymbol{y}] \quad (7)$$

Therefore, the only assumption on the measurement uncertainties is that they are bounded. No additional assumptions, e.g. about their stochastic properties, are necessary. Furthermore, we assume

$$\boldsymbol{u}(t) \in [\boldsymbol{u}(t_k)]\ \forall t \,|\, t_k \leq t < t_{k+1}, \quad (8)$$

i.e. $[\boldsymbol{u}(t_k)]$ is a piecewise constant interval vector. This can always be achieved by appropriate selection of $\Delta\boldsymbol{u}$.

By using interval-valued parameters in $[\boldsymbol{f}(\cdot)]$, model uncertainties can be taken into account. This includes parametric uncertainties as well as non-modeled system dynamics as long as their effects can be described by parameter variations smaller than the considered parametric uncertainties.

The model and measurement uncertainties result in a set of possible states represented by the interval state vector $[\boldsymbol{x}]$.

3. STATE-SET OBSERVER

Traditional state observers aim at reconstructing the system state based on measurement information using a feedback structure resulting in stable error dynamics. Using concepts e.g. based on Kalman filtering, noise effects with known stochastic properties can be taken into account.

By contrast, the state-set observer proposed in this contribution is based on uncertain measurements where the uncertainty is bounded (see (6) and (7)). Except these bounds no further information about the type of uncertainty is required.
By using interval system models, model uncertainties in the form of interval-valued parameters can also be accounted for. This can significantly reduce the modeling overhead while still leading to satisfying diagnosis results.

The state-set observer follows the well-known predictor-corrector scheme:

(1) During the **prediction step**, a predicted state set $\mathcal{X}_p(t_{k+1})$ is calculated with a validated ODE solving algorithm based on the system differential equation and the previous consistent state set $\mathcal{X}(t_k)$.

(2) In the subsequent **correction step**, the predicted state set is updated using the available measurements of the output variables $\boldsymbol{y}(t_{k+1})$. Note that due to the continuous-time approach, measurements need not necessarily be obtained using a constant sample time.

Both the prediction and the correction step are explained in detail below.

3.1 Prediction Step

For calculation of the predicted state set $\mathcal{X}_p(t_{k+1})$ from the previous consistent state set $\mathcal{X}(t_k)$, the validated ODE solving algorithm developed in Nedialkov (1999) is extended to the case of non-autonomous systems. The algorithm is based on a Taylor series expansion of the system function $\boldsymbol{f}(\cdot)$ from (5) with respect to time up to an arbitrary order chosen by the user. This order is also called the order of the observer. The coefficients of the Taylor series are determined by automatic or algorithmic differentiation (see e.g. Griewank (2000) for details). This means that only the system function $\boldsymbol{f}(\cdot)$ itself and no derivatives must be supplied by the user. All calculations are done in interval arithmetic for proper handling of state sets as well as roundoff errors and Taylor series remainders.

The algorithm was originally developed for guaranteed simulation of autonomous systems. It is extended here to account for piecewise constant interval input vectors as described in Section 2. Since $[\boldsymbol{u}(t_k)]$ is assumed constant in the time interval covered by one prediction step, it can be seen as a constant interval-valued parameter of the system function. In this way, input signals that are enclosed in piecewise constant intervals can be handled using the original validated algorithm.

The algorithm consists of two parts:

(a) Calculation of an initial set $\mathcal{X}([t_k, t_{k+1}])$ enclosing all continuous trajectories emanating from $\mathcal{X}(t_k)$ for the time interval $[t_k, t_{k+1}]$ (see Fig. 1a).
(b) Calculation of a tight enclosure of the state set at the desired time instant t_{k+1}, which represents the predicted state set $\mathcal{X}_p(t_{k+1})$ of the observer. For reasons explained below, the predicted set comprises two different set representations (see Fig. 1b).

Part (a) calculates the interval Taylor series coefficients by automatic differentiation in interval arithmetic, including an interval that encloses the Taylor series remainder. These intervals are reused in part (b) to guarantee that the true state set is enclosed. For the time interval $[t_k, t_{k+1}]$, an enclosure of the continuous state trajectories emanating from each point of the initial state set $\mathcal{X}(t_k)$ is calculated as indicated in Fig. 1a. Using interval arithmetic, this can be accomplished directly without having to consider any of these trajectories specifically.
Mathematically speaking, this proves the existence and uniqueness of the solution of the interval initial value problem.

Part (b) uses the results from part (a) to calculate two different enclosures of the true state set at t_{k+1}:

(i) An interval vector $[\boldsymbol{x}]$ representing an axis-aligned box.

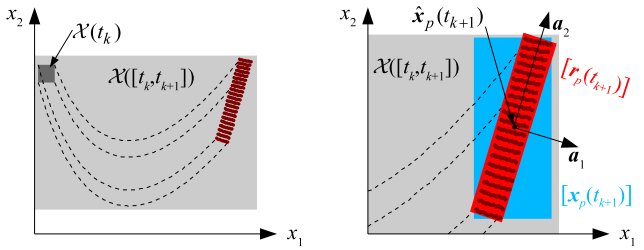

(a) trajectory enclosure (b) predicted set enclosures

Fig. 1. Two-dimensional illustration of the two parts of the prediction step

(ii) A rotated interval set $\hat{\boldsymbol{x}} + \boldsymbol{A}\,[\boldsymbol{r}]$, where $\hat{\boldsymbol{x}}$ is the midpoint of $[\boldsymbol{x}]$, $\boldsymbol{A}$ is an orthogonal matrix and $[\boldsymbol{r}]$ is an interval vector representing the rotated state set in the coordinate system induced by $\boldsymbol{A}$.

The main reason for the calculation of the second representation is the reduction of the overestimation of the true state set. This overestimation occurs since the true state set must be wrapped in a larger set whose representation is suitable for subsequent calculations. More details on the implementation of the validated algorithm can be found in Nedialkov (1999).

Since both sets $[\boldsymbol{x}]$ and $\hat{\boldsymbol{x}} + \boldsymbol{A}\,[\boldsymbol{r}]$ are calculated such that they guarantee to enclose the true state set, the desired predicted state set is the intersection of these two sets:

$$\mathcal{X}_p(t_{k+1}) = [\boldsymbol{x}_p(t_{k+1})] \cap \left(\hat{\boldsymbol{x}}_p(t_{k+1}) + \boldsymbol{A}_p(t_{k+1})\,[\boldsymbol{r}_p(t_{k+1})]\right) \tag{9}$$

Since interval arithmetic is used in all calculations, $\mathcal{X}_p(t_{k+1})$ includes all roundoff errors as well as the Taylor series remainder term. Furthermore, since the algorithm allows to include interval-valued input variables and system parameters, this approach does indeed guarantee that the calculated state set encloses the true state set if the assumptions on the system model and the uncertainties are correct. This property makes the described approach superior to other set-valued approaches that rely on approximate nonlinear discrete-time descriptions of the system dynamics.

3.2 Correction Step

The state set $\mathcal{X}_p(t_{k+1})$ calculated in the prediction step is consistent with the system model including model and input uncertainties. In the correction step, the predicted set can be tightened using the available uncertain measurements $[\boldsymbol{y}(t_{k+1})]$. As stated in Section 2, we restrict our considerations to the case where the elements of the output vector equal the first q state variables (5). This results in a *measured set* $\mathcal{X}_m(t_{k+1})$, i.e. a set of states consistent with the output measurements:

$$\mathcal{X}_m(t_{k+1}) = \left(\left[\boldsymbol{y}^{\mathrm{T}}(t_{k+1})\right], [-\infty, \infty], \ldots, [-\infty, \infty]\right)^{\mathrm{T}} \tag{10}$$

The consistent state set $\mathcal{X}(t_{k+1})$ for the next iteration of the set-valued observer is the intersection of the predicted and the measured state set.

To proceed to the next iterations' prediction step, the intersection set must be described in the same form as $\mathcal{X}_p(t_{k+1})$ in (9). Such a representation can be calculated by an interval Gauss-Seidel algorithm (see Neu-

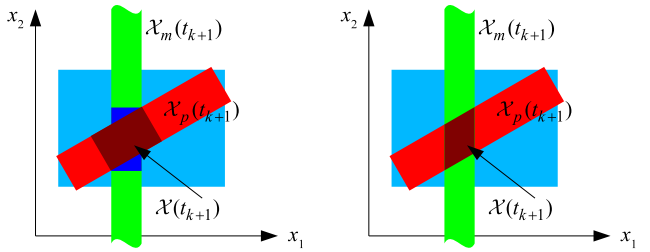

(a) result of the Gauss-Seidel algorithm (b) additional modification of $\boldsymbol{A}(t_{k+1})$

Fig. 2. State set correction by intersection of the predicted and the measured set, x_1 is measured

maier (1990)) resulting in tighter interval vectors $[\boldsymbol{x}(t_{k+1})]$ and $[\boldsymbol{r}(t_{k+1})]$, but leaving the orthogonal Matrix $\boldsymbol{A}$ unchanged, that is $\boldsymbol{A}(t_{k+1}) = \boldsymbol{A}_p(t_{k+1})$ (see Fig. 2a). This yields the following correction algorithm:

(1) Use the measurement information to calculate a tighter interval vector $[\bar{\boldsymbol{x}}(t_{k+1})]$:
$$[\bar{\boldsymbol{x}}(t_{k+1})] = [\boldsymbol{x}_p(t_{k+1})] \cap \mathcal{X}_m(t_{k+1}) \tag{11}$$
(2) Use the interval Gauss-Seidel algorithm to calculate $[\bar{\boldsymbol{r}}(t_{k+1})]$ from
$$[\bar{\boldsymbol{x}}(t_{k+1})] = \hat{\boldsymbol{x}}_p(t_{k+1}) + \boldsymbol{A}(t_{k+1})\,[\bar{\boldsymbol{r}}(t_{k+1})]\,. \tag{12}$$
Note that $\boldsymbol{A}(t_{k+1})$ is an orthogonal non-interval matrix and no preconditioning is required in this step. Due to the properties of interval arithmetic, the Gauss-Seidel algorithm in general gives much better results than directly solving (12) for $[\bar{\boldsymbol{r}}(t_{k+1})]$.
(3) Calculate $[\boldsymbol{x}(t_{k+1})]$ from
$$[\boldsymbol{x}(t_{k+1})] = [\bar{\boldsymbol{x}}(t_{k+1})] \cap \big(\hat{\boldsymbol{x}}_p(t_{k+1}) + \boldsymbol{A}(t_{k+1})\,[\bar{\boldsymbol{r}}(t_{k+1})]\big). \tag{13}$$
This step tightens the non-measurable elements of $[\boldsymbol{x}(t_{k+1})]$.
(4) Calculate the new midpoint $\hat{\boldsymbol{x}}(t_{k+1})$ of $[\boldsymbol{x}(t_{k+1})]$ and account for the offset by
$$[\boldsymbol{r}(t_{k+1})] = [\bar{\boldsymbol{r}}(t_{k+1})] + \big[\boldsymbol{A}^{-1}(t_{k+1})\big]\,\big(\hat{\boldsymbol{x}}_p(t_{k+1}) - \hat{\boldsymbol{x}}(t_{k+1})\big). \tag{14}$$
Note that $\big[\boldsymbol{A}^{-1}(t_{k+1})\big] = \big[\boldsymbol{A}^{\mathrm{T}}(t_{k+1})\big]$ is an interval matrix enclosing the inverse of the orthogonal matrix $\boldsymbol{A}(t_{k+1})$ to account for the roundoff error.

Due to the properties of interval arithmetic and $\boldsymbol{A}(t_{k+1})$ being an orthogonal real-valued matrix, this procedure results in tight bounds on $[\boldsymbol{x}(t_{k+1})]$ and $[\boldsymbol{r}(t_{k+1})]$ in one single iteration of this algorithm.

As obvious from Fig. 2a, both representations of the consistent state set extend beyond the true intersection set. Although this is not a problem for many applications, even better results can be achieved by appropriate modification of $\boldsymbol{A}(t_{k+1})$. Since the next prediction step does not require $\boldsymbol{A}(t_{k+1})$ to be an orthogonal matrix, we can use a modified matrix $\tilde{\boldsymbol{A}}(t_{k+1})$ such that the representation in the form given by (9) describes the smallest possible parallelepiped enclosing the true intersection set (see Fig. 2b).

To obtain such a suitable matrix $\tilde{\boldsymbol{A}}(t_{k+1})$, we need to find n column vectors $\tilde{\boldsymbol{a}}_i^{\mathrm{T}}$ and n intervals $[\tilde{r}_i]$ such that the parallelepiped described by $\tilde{\boldsymbol{A}}(t_{k+1})\,[\tilde{\boldsymbol{r}}(t_{k+1})]$ has minimal volume. The $2n$ column vectors of $\big(\boldsymbol{I}_n,\ \boldsymbol{A}^{-1}(t_{k+1})\big)$ are the normal vectors defining the supporting hyperplanes of the regarded parallelepiped. Finding the desired column vectors of $\tilde{\boldsymbol{A}}(t_{k+1})$ thus merely amounts to selecting n of these $2n$ vectors and using them as row vectors of $\tilde{\boldsymbol{A}}^{-1}(t_{k+1})$ to calculate the new base matrix $\tilde{\boldsymbol{A}}(t_{k+1})$. This task is carried out by simple enumeration of all possible combinations and selecting the one combination resulting in a minimal parallelepiped volume.
The required intervals $[\tilde{\boldsymbol{r}}(t_{k+1})]$ can then be calculated by
$$[\tilde{\boldsymbol{r}}(t_{k+1})] = \Big(\Big[\tilde{\boldsymbol{A}}^{-1}(t_{k+1})\Big]\,\boldsymbol{A}(t_{k+1})\Big)\,[\boldsymbol{r}(t_{k+1})] \cap \Big[\tilde{\boldsymbol{A}}^{-1}(t_{k+1})\Big]\,\big([\boldsymbol{x}(t_{k+1})] - \hat{\boldsymbol{x}}(t_{k+1})\big). \tag{15}$$
While more sophisticated algorithms could be developed for this task, even this relatively simple approach shows the performance of the method.

Regarding the result of this correction algorithm, two cases must be distinguished: An empty intersection set means that the real system behavior is inconsistent with the system model and the assumptions on the measurement and model uncertainties. A non-empty intersection set is guaranteed to contain all system states consistent with the system model and all present and past measurements including uncertainties. This property makes this set-valued observer particularly well-suited for robust consistency-based diagnosis algorithms.

4. CONSISTENCY-BASED DIAGNOSIS ALGORITHM

The basic idea of consistency-based diagnosis methods is to check whether the behavior of the real system is consistent with the behavior of mathematical system models. These consistency tests are designed such that faulty system behavior can be detected as well as different faults can be isolated. In Planchon (2007), a consistency-based diagnosis algorithm for linear discrete-time systems was developed. This algorithm is extended here to the case of nonlinear, continuous-time systems.

Similar to Planchon (2007), we consider a set of *fault candidates*
$$\mathcal{F} = \{F_0, F_1, F_2, \dots\} \tag{16}$$
with associated system models $\mathcal{M}_{F_i}$ of the form (5). Each fault candidate describes the behavior of the system subject to a single abrupt or incipient fault. The fault-free candidate is given by F_0, the candidates F_1, F_2, ... represent different faults to be isolated with the help of the diagnosis algorithm. Note that for fault detection only the fault-free candidate F_0 is required, while the task of fault isolation requires a candidate for each characteristic fault to be isolated.

For each system model $\mathcal{M}_{F_i}$, a set-valued observer is designed which is initialized with an arbitrary state set fulfilling the requirement that the true initial system state is contained in this set. Starting with this initial state set, the observer calculates a state set at a desired time instant (usually a time instant where measurements are available). This set is consistent with both, the system model and the measurements including all uncertainties.

If the assumptions, i.e. the system models including uncertainties, are correct, it directly follows from the observer properties that the true system state is **guaranteed** to be

contained in the calculated state set. On the other hand, if the assumptions on the measurement uncertainties are correct and the observer fails to find a consistent state set (resulting in an empty state set), it can be concluded that the respective system model cannot correctly describe the true system behavior given by the available measurements.

Therefore, in each iteration, the result of the set-valued observer for each fault candidate in $\mathcal{F}(t_k)$ is checked for an empty state set. The candidates F_i with empty state sets are not included in the set of fault candidates $\mathcal{F}(t_{k+1})$ since the corresponding system models $\mathcal{M}_{Fi}$ cannot describe the true system behavior. Hence, each element in $\mathcal{F}(t_{k+1})$ describes a fault that **can have** occurred. On the other hand, we can guarantee that faults yielding an empty set have **not** occurred, thus the algorithm does not produce false alarms.

From this, we can conclude the following:

- If the fault-free system model $\mathcal{M}_{F_0}$ results in an empty state set, the behavior of the real system is not consistent with the fault-free behavior meaning that some fault must have occurred (*fault detection*).
- If there remains only one element F_i in the set of fault candidates $\mathcal{F}$, then it can be concluded that the corresponding fault has occurred (*fault isolation*). Note that it is possible that multiple elements F_i remain in $\mathcal{F}$ if the corresponding models describe faults that cannot be isolated (partial fault isolation). It is also possible that $\mathcal{F}$ is an empty set if not all possible faults are modeled and such an unmodeled fault has occurred.

Since both, model and measurement uncertainties can be accounted for, a robust fault detection and isolation scheme can be implemented with the following algorithm:

(1) Initialize the set of fault candidates $\mathcal{F}(t_0)$ with all fault candidates F_i.
(2) Initialize each observer with an initial state set $\mathcal{X}(t_0)$ that contains the true initial system state.
(3) For each element in $\mathcal{F}(t_k)$, calculate the subsequent consistent state set $\mathcal{X}(t_{k+1})$.
(4) Build $\mathcal{F}(t_{k+1})$ using all system models with a non-empty state set $\mathcal{X}(t_{k+1})$.
(5) **If** $F_0 \notin \mathcal{F}(t_{k+1})$**:**
Fault detected, for fault isolation restart with step (1). F_0 can be omitted.
If $\mathcal{F}(t_{k+1}) = \{F_i\} \neq \{F_0\}$**:**
Fault isolated, stop.
Else:
Proceed to the next iteration with step (3).

The nonlinear state-set observer described in Section 3 can be used for combined state and parameter estimation. While this can significantly reduce the number of fault candidates required for fault isolation and allows to handle incipient faults, the "empty-set criterion" may no longer be sufficient for good diagnosis results in some cases. In this case, the diagnosis algorithm must be extended by additional FDI criteria, e.g. one can conclude that a fault has occurred if the consistent interval for some system parameter does no longer contain the known nominal parameter value. However, such extensions to the diagnosis algorithm require further research.

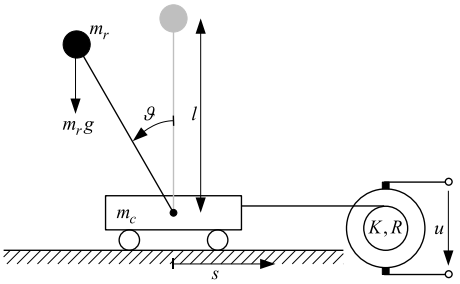

Fig. 3. The inverted pendulum

5. APPLICATION EXAMPLE

The performance of the proposed diagnosis algorithm is demonstrated using real measurement data from an inverted pendulum. After a short description of the pendulum and its system model, the diagnosis results are presented.

5.1 The Inverted Pendulum

Fig. 3 shows a sketch of the inverted pendulum used to obtain the measurement data. It consists of a DC-motor-driven cart mounted on a rail with an attached rod able to perform full rotations. Such a pendulum is a widely-used benchmark system in the control systems world. The strong nonlinearity as well as the unstable upper equilibrium point also make it an excellent benchmark for the proposed diagnosis algorithm and the set-valued observer.

Using the state vector $\boldsymbol{x} = \left(s \;\; \vartheta \;\; \dot{s} \;\; \dot{\vartheta}\right)^{\mathrm{T}}$, the pendulum motion can be described by the system model

$$\begin{cases} \dot{\boldsymbol{x}} &= \left(\dot{s} \;\; \dot{\vartheta} \;\; \ddot{s} \;\; \ddot{\vartheta}\right)^{\mathrm{T}} \\ \boldsymbol{y} &= \left(s \;\; \vartheta\right)^{\mathrm{T}} \end{cases} \tag{17}$$

with

$$\ddot{s} = \frac{m_r \sin\vartheta \left(g\cos\vartheta - l\dot{\vartheta}^2\right) - \frac{K^2}{R}\dot{s} + \frac{K}{R}u}{m_c + m_r \sin^2\vartheta} \quad \text{and}$$

$$\ddot{\vartheta} = \frac{\left(\frac{K}{Rl}u - m_r\dot{\vartheta}^2 \sin\vartheta - \frac{K^2}{Rl}\dot{s}\right)\cos\vartheta + \frac{g(m_c+m_r)}{l}\sin\vartheta}{m_c + m_r \sin^2\vartheta}.$$

In this model, the rod is described by a point mass m_r at distance l from the center of rotation. The parameters m_c, K and R denote the cart mass, the motor constant and the armature resistance of the DC motor, respectively. The input variable is the armature voltage u in the range $\pm 5\,\mathrm{V}$.

The system is operated using a discrete-time controller with a constant sample time of $T = 0.01\,\mathrm{s}$. Thus, the requirement of piecewise constant input variables is fulfilled.

5.2 Diagnosis Results

To demonstrate the performance of the proposed diagnosis algorithm, three different operation modes are regarded:

F_0: fault-free (nominal) operation
F_1: additional mass attached to the rod
F_2: additional mass attached to the cart

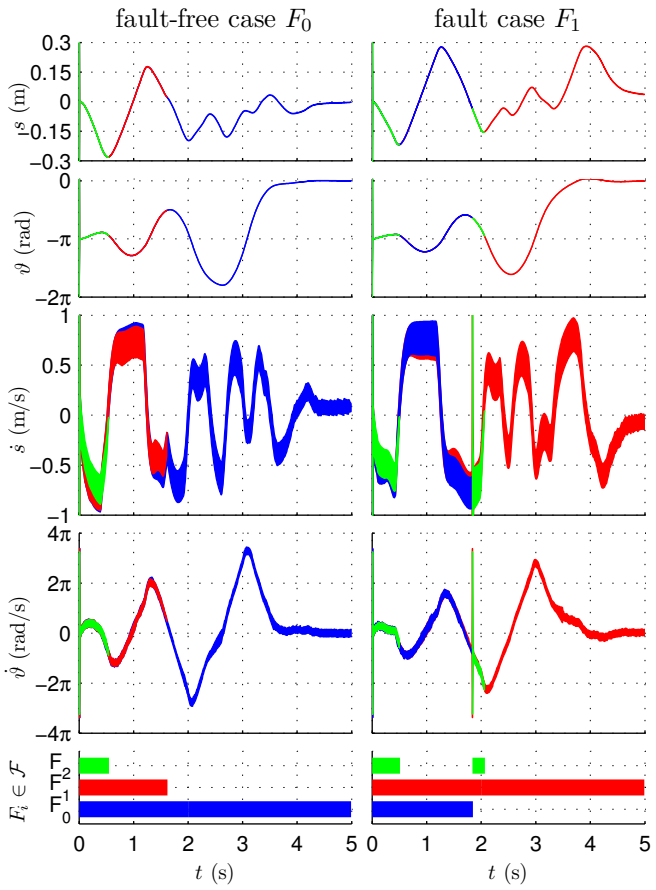

Fig. 4. Diagnosis results for the inverted pendulum

The parameters of the fault-free system model $\mathcal{M}_{F_0}$ are

$$[m_c] = [1.158, 1.160]\ \text{kg} \qquad [K] = [5.35, 5.45]\ \text{Nm/A}$$
$$[m_r] = [0.343, 0.345]\ \text{kg} \qquad [R] = [2.6, 2.8]\ \Omega$$
$$[l] = [0.423, 0.425]\ \text{m} \qquad [g] = [9.80, 9.82]\ \text{m/s}^2.$$

The mass attached to the rod results in a different equivalent length $[l] = [0.505, 0.510]\,\text{m}$ and rod mass $[m_r] = [0.420, 0.425]\,\text{kg}$ for the model $\mathcal{M}_{F_1}$. The mass attached to the cart yields a cart mass of $[m_c] = [2.0, 2.05]\,\text{kg}$ for the model $\mathcal{M}_{F_2}$. All other parameters of $\mathcal{M}_{F_1}$ and $\mathcal{M}_{F_2}$ are equal to those of $\mathcal{M}_{F_0}$.

The input uncertainty includes unmodeled friction effects and is assumed to be $\Delta u = 0.3\,\text{V}$. The output measurement uncertainties are $\Delta \boldsymbol{y} = (0.001\,\text{m},\ 0.002\,\text{rad})^{\mathrm{T}}$.

For the three system models $\mathcal{M}_{F_0}$, $\mathcal{M}_{F_1}$ and $\mathcal{M}_{F_2}$, a set-valued observer of order 5 as described in Section 3 is implemented and initialized with the initial state set

$$\mathcal{X}(t_0) = [\boldsymbol{a}] \cap (\boldsymbol{0} + \boldsymbol{I}_4\ [\boldsymbol{a}]) \tag{18}$$

with $[\boldsymbol{a}] = ([-0.7, 0.7]\,,\ [-2\pi, 2\pi]\,,\ [-1, 1]\,,\ [-3\pi, 3\pi])^{\mathrm{T}}$. Note that an initial measurement could be used to obtain tighter initial intervals for the measurable state variables.

Fig. 4 shows the results of the diagnosis algorithm for the fault-free case F_0 (left) and the fault case F_1 (right). Despite the relatively large input uncertainty and the large inital state set, the set-valued observer converges rapidly and yields very tight bounds on the non-measurable state variables.

In the fault-free case, only F_0 remains in $\mathcal{F}$ while both fault models $\mathcal{M}_{F_1}$ and $\mathcal{M}_{F_2}$ yield empty sets. Therefore, after approximately 1.6 s, the (correct) conclusion is reached that no fault has occurred.
In the faulty case the fault-free system model yields an empty set after approximately 1.9 s, which gives the conclusion that a fault must have occurred. After re-initialization for fault isolation only F_1 remains in $\mathcal{F}$, hence the conclusion is reached that fault F_1 has occurred.

In general, the amount of time needed for fault detection and isolation after the occurrence of a fault is related to the fault strength as well as the amount of uncertainty in the system models. Despite the large input uncertainty, here it is possible to detect and isolate a fault in about 2 seconds.

6. CONCLUSION

The proposed diagnosis algorithm allows to detect and isolate faults of continuous-time nonlinear systems with discrete measurements in the presence of uncertainties, which are inevitable in models of real technical systems. It is therefore a powerful tool for model-based diagnosis yielding robust results with limited modeling effort. If the assumptions on the system models and the uncertainties are correct, no false alarms can occur. The performance of the approach was shown using an inverted pendulum.
Further research directions include convergence properties of the proposed set-valued observer as well as combined state and parameter estimation.

REFERENCES

J. Chen and R.J. Patton. *Robust Model-Based Fault Diagnosis for Dynamic Systems.* Kluwer Academic Publishers, Boston, USA, 1999.

A. Griewank. *Evaluating Derivatives: Principles and Techniques of Algorithmic Differentiation.* SIAM, Philadelphia, USA, 2000.

U.D. Hanebeck. Recursive nonlinear set-theoretic estimation based on pseudo-ellipsoids. *Proc. of IEEE MFI Conference, Baden-Baden, Germany*, 2001.

L. Jaulin, M. Kieffer, O. Didrit, and E. Walter. *Applied Interval Analysis.* Springer, London, UK, 2001.

N.S. Nedialkov. *Computing Rigorous Bounds on the Solution of an Initial Value Problem for an Ordinary Differential Equation.* Ph.D. thesis, University of Toronto, Toronto, Canada, 1999.

A. Neumaier. *Interval Methods for Systems of Equations.* Cambridge University Press, Cambridge, UK, 1990.

R.J. Patton, P.M. Frank, and R.N. Clark. *Issues of Fault Diagnosis for Dynamic Systems.* Springer, London, UK, 2000.

P. Planchon. *Guaranteed Diagnosis of Uncertain Linear Systems using State-Set Observation.* Logos Verlag, Berlin, Germany, 2007.

V. Puig, J. Quevedo, and S. Tornil. Robust fault detection: Active versus passive approaches. *IFAC SAFEPROCESS Hungary*, 2000.

V. Puig, J. Quevedo, T. Escobet, and S. de las Heras. Passive robust fault detection approaches using interval models. *IFAC World Congress, Barcelona, Spain*, 2002.

J.S. Shamma and K-Y. Tu. Approximate set-valued observers for nonlinear systems. *IEEE Trans. on Automatic Control*, 42:648–658, 1997.